Some Basic Graphic Guidelines

Some Basic Graphic Guidelines > >

Images should guide the overall layout, not the text.

Some Basic Graphic Guidelines > >

Avoid cluttering the poster (graphs, photos, etc.).

Some Basic Graphic Guidelines > >

Watch your color contrasts.

Some Basic Graphic Guidelines > >

Make sure all components are aligned properly.

Our compiling strategy is to exploit coarse-grain parallelism at function application level: and the function application level parallelism is implemented by fork-join mechanism. The compiler translates source programs into control flow graphs based on analyzing flow of control, and then serializes instructions within graphs according to flow arcs such that function applications, which have no control dependency, are executed in parallel.

We describe the philosophy and design of the control flow machine, and present the results of detailed simulations of the performance of a single processing element. Each factor is compared with the measured performance of an advanced von Neumann computer running equivalent code. It is shown that the control flow processor compares favorably in the program.

We present a denotational semantics for a logic program to construct a control flow for the logic program. The control flow is defined as an algebraic manipulator of idempotent substitutions and it virtually reflects the resolution deductions. We also present a bottom-up compilation of medium grain clusters from a fine grain control flow graph. We compare the basic block and the dependence sets algorithms that partition control flow graphs into clusters.

We have demonstrated that to achieve the best execution time for a control flow program, the number of nodes within the system and the type of mapping scheme used are particularly important. In addition, we observe that a large number of subsystem nodes allows more actors to be fired concurrently, but the communication overhead in passing control tokens to their destination nodes causes the overall execution time to increase substantially.

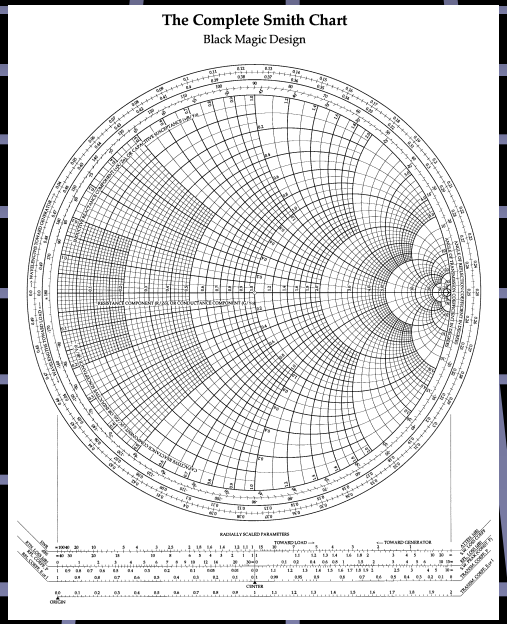

We apply a parallel simulation scheme to a real problem: the simulation of a control flow architecture, and we compare the performance of this simulator with that of a sequential one. Moreover, we investigate the effect of modeling the application on the performance of the simulator. Our study indicates that parallel simulation can reduce the execution time significantly if appropriate modeling is used.

Some Text Guidelines

Some Text Guidelines > >

- Break text up with bullets or...

1. numbers

Some Text Guidelines > >

- Indenting shows subordination
  - As in this example

Some Text Guidelines > >

Avoid lengthy paragraphs talking about why you did what you did and whether you dislike positivism because there is such a thing as reality out there and it operates in a certain way and we should be able to access that in some shape, form, or fashion and besides it's all from some stuffy old dead guy thinking too hard, anyway.

Some Text Guidelines > >

Be sure your letters stand out against the background.

Some Text Guidelines > >

Use fonts people can read.
Titles/headings: 40 to 80pt
Body text: no less than 16 pt

Some Text Guidelines > >

TRIM EVERYTHING THAT'S NOT DIRECTLY PERTINENT

Some Text Guidelines > >

Fat Text — to — Lean Text

- Teeth are ideal for studying life history because they grow incrementally, are not remodeled during an individual's lifetime, and are not highly subject to environmental stresses.

Some Text Guidelines > >

Fat Text — to — Lean Text

- Teeth are ideal for studying life history because they grow incrementally, are not remodeled during an individual's lifetime, and are not highly subject to environmental stresses.

- **Teeth & Life History**
  - Incremental growth
  - Not remodeled
  - Resistant to environmental stress

Standard Outline

Title
Introduction
Results
Discussion
Conclusion
References and acknowledgments

Some Standard Templates

Left to Right, Top to Bottom Flow

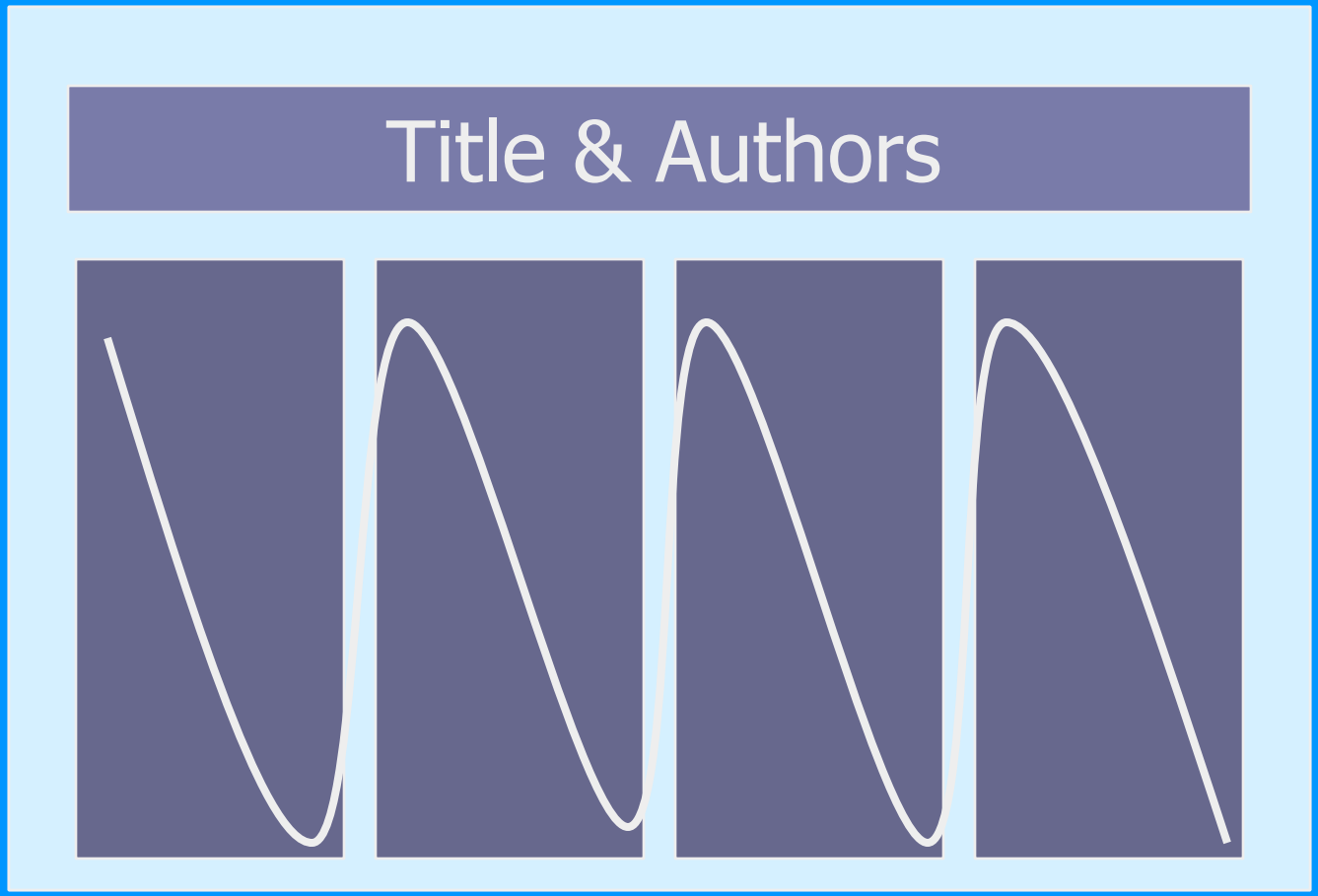

Left to Right Flow in Rows

Title & Authors

Part 1

Part 2

Part 3

Centered Image & Peripheral Explanations

Title & Authors

Centered Explanation, Peripheral Images

Title & Authors

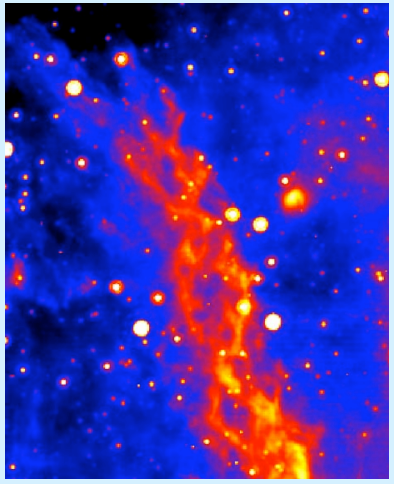

Automatic paralogous gene detection and structural annotation of multigene families: application to the MYB family of transcription factors in *Arabidopsis thaliana*.

Jeroen Raes[1,2], Sébastien Aubourg[3], Patrice Dehais[1] and Pierre Rouzé[1,2]

[1] Department of Plant Genetics, Flanders Interuniversity Institute for Biotechnology (VIB), University of Ghent, Ghent, Belgium
[2] Laboratoire associé de l'INRA, University of Ghent , Ghent, Belgium
[3] Current affiliation: Unité de Recherche en Génomique Végétale, INRA, Evry, France

Introduction

Now that more and more full genome sequences become available, the possibilities for evolutionary research seem endless: one can collect all members of a gene family, without missing the low or conditionally expressed ones, which was often the case in cDNA-library based family studies. Unfortunately, having the complete genome is only the beginning: the automatic annotation done by the large sequencing consortia is often of poor quality[1]. As such, it is very unlikely that a perfect and exhaustive set of family members can be collected just by using the family name as query in a search engine (e.g. SRS).

To avoid the tedious task of manually correcting structural and functional annotation, we developed a method that allows us to retrieve exhaustively all family members given a representative set (e.g. of experimental origin) and a set of genomic (e.g. BAC) sequences. The final result of this routine consists of the gene structure, position and mRNA/protein sequence of all the family members.

This method was applied to the Myb family of transcription factors in the *Arabidopsis thaliana* genome.

Methodology

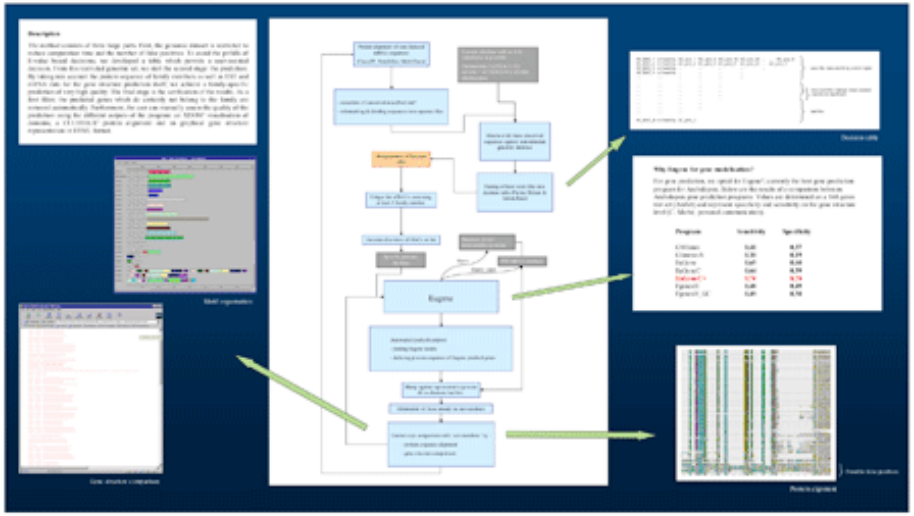

Application

The Myb family of transcription factors is one of the largest families in *Arabidopsis thaliana*. They are implicated in various processes, such as secondary metabolism, cellular morphogenesis, growth regulator response signalling, etc[4]. This diversity of functions, combined with an explosive expansion of this family in comparison to animals (e.g. Humans have only 3 known Mybs), make this family very interesting for gene family evolution studies. As a family, it is not of the easiest to detect: the only conserved area is a 50aa sequence which is repeated (degenerately) up to three times. At the genomic level, the repeats are usually interrupted by an intron, which increases the detection difficulty even further.

From a set of 24 representative R2-R3 Myb subfamily members, ±140 R2-R3 Mybs were found in the Arabidopsis genome, which is in agreement with a recent study done on Arabidopsis transcription factors[5]. In more than 90% of the cases, the comparison to the other family members allowed us to decide that the automated gene structure prediction was correct.

References: 1. Aubourg,S. and Rouzé,P. (2000), Plant Physiol. Biochem. 39, 1-13 2. Geourjon C. et al. (1997) Comput Appl Biosci.13(6), 681-8 3. Thompson, J.D. et al. (1997) Nucleic Acids Research 24, 4876-82 4. Schütz, T. et al. JOBIM'2000 (Journées Ouvertes Biologie Informatique Mathématiques). To appear in LNCS. 5. Martin, C. and Paz-Ares, J. (1997) TIG 13(2), 67-73 6. Riechmann J.L. et al. (2000) Science 15;290(5499), 2105-10

Baby Frankenstein, or Doing What's Best for Your Child?

Baruch College, Professor Schulman, Jonathan Jordan, Ryan Weidman, Alyssa Wick, Kateryna Kuntsevich

Abstract

When you and your significant other are ready to have a child, will you make the conscious decision to have a disease free child, or will you stick with the luck of the draw? With Pre-implantation Genetic Diagnosis, it is possible to make that decision. Helping to fight genetic diseases and conditions, PGD is a process that began about 10 years ago, in which an embryo is scanned for genetic diseases. The disease free embryos are implanted and the unwanted ones are discarded. The negative aspects of PGD include the creation of "designer babies," "sibling saviors" and a genetic class-divide. In our poster we have discussed both the positive and negative ideals that have developed around PGD, as well as how this procedure can be used ethically and effectively to improve our society's health, and possibly change the view of disease in general. PGD is not a thing of the future, it is happening right now!

PGD Overview

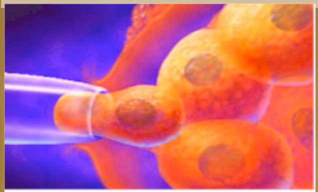

Blastomere Biopsy & Preimplantation genetic diagnosis (PGD). PGD is performed as a part of an In Vitro Fertilization cycle where multiple embryos are available. At their earliest stage of development, one cell is removed from each morula through a procedure called embryo biopsy. These cells are analyzed in the PGD Laboratory to determine which embryos are free of genetic abnormalities so they can be transferred to the uterus.

http://www.fertilityproregistry.com/content/pgd_sex_selection.asp

Relative Success Rates:

Success rates depend on the center/clinic performing PGD.

*29% pregnancy rate per oocyte retrieval and 38% per embryo transfer (10)

*The Guy's and St Thomas' Centre for PGD has a success rate of 19% per oocyte retrieval and 29% per embryo transfer (10)

*ESHRE Consortium reports 16.8% per oocyte retrieval and 21.4% per embryo transfer (10)

*32% pregnancy rate per patient, compared to 32% in natural conception (6).

Also, some research has found that the success rate of the first cycle of PGD is indicative of the success rate of the 2nd and 3rd cycles, as seen in the graph below. The success rate of the first cycle is the lowest, so if it fails, then the chances of having a successful pregnancy only increase.

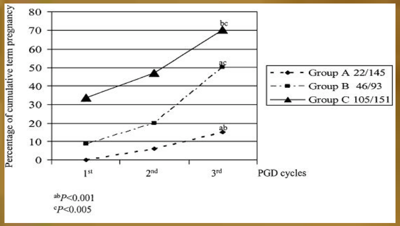

$^{ab}P<0.001$
$^{c}P<0.005$

http://www.wisc.edu/ansci_repro/misc/project_websites_06/wednesday/human_art/ART%20website.htm

Arguments in support of PGD

- Couples are able to bear children knowing that the child will not have to suffer with a disease that is common in the family.
- Keeps couples from having abortions after amniocentesis.
- Some children are born with awful and deadly diseases that can only be treated with a transplant from an exact match. Parents are using PGD to find that match, instead of conceiving naturally and aborting after finding out the fetus either isn't a match, or also has the disease.
- Some feel that PGD for gender selection would be alright in the case of family balancing, that is, wanting to have a male after three females, or the other way around.

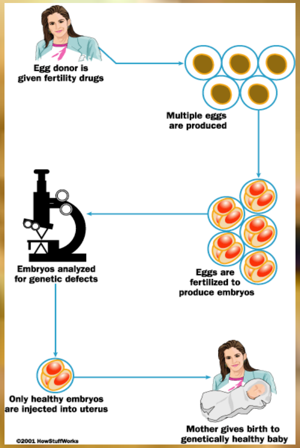

Arguments against use of PGDs

- In this process, a lot of embryos are simply discarded (sometimes frozen, but not usually used later). Some would say this is a type of murder because they believe that embryos are human life.
- There is a question of whether or not excluding an embryo because of the possibility of developing a disease or impairment is discrimination.
- For those siblings who were born using PGD, simply because they were a match, is it fair? It is quite possible that they will develop a sort of inferiority complex when they learn of their purpose in life. Also, if the transplant doesn't work, will the parents blame the sibling and resent him/her for it?
- A large fear that comes from PGD is that the world will turn into one of designer children. It will be like everyone is manufactured, not created and could lead to even more people feeling poorly about themselves because they are not perfect.
- Since it is such a specialized procedure, it is very costly. This could increase the gap between the wealthy and the poor, because the rich will be able to be sure their children are disease free, whereas the poor will not

Procedure	Cost in Dollars
Processing and Insemination per month	300 – 700
Ovulation Induction by Injection	1000 – 4,000
Ovulation Induction by Oral Pills	50 – 700
Three Months of treatment without ovulation Induction	900 – 2,100
Three Months of treatment with Ovulation Inductions	1,900 – 6,100
Six Months of treatment without Ovulation Inductions	1,800 – 4,200
Six Months of treatment with Ovulation Induction	3,800 – 12,200

PGD in New York City

- The Center for Reproductive Medicine and Infertility at New York Presbyterian Hospital, Weill-Cornell Medical Center, New York City
  - Number of ART cycles and transfers in 2002: 2,012
  - Percentage of ART cycles from non-donor fresh embryos resulting in live births in 2002: 48% (under age 35), 43% (ages 35-37), 30% (ages 38-40), 18% (ages 41-42)
  - Is one of the most experienced centers in the U.S., with 11,000-plus babies born through conventional IVF and 4,000 through ICSI -- a technique that injects a single sperm into an egg; ICSI, invented by the center's lab director, is a must for couples with severe male factor infertility
  - Performed the first genetic testing on embryos for sickle cell anemia and retinoblastoma, an inherited eye cancer
- New York University School of Medicine, Program for In-Vitro Fertilization, Reproductive Surgery, and Infertility, New York City
  - Number of ART cycles and transfers in 2002: 1,362
  - Percentage of ART cycles from non-donor fresh embryos resulting in live births in 2002: 45% (under age 35), 42% (ages 35-37), 24% (ages 38-40), 17% (ages 41-42)
  - about 70% of patients have failed at least one IVF cycle elsewhere
  - Offers a patient library equipped with computers
  - Is developing an egg-freezing program

The Arabidopsis group,
Department of
molecular biosciences
University of Oslo

MARC
The Norwegian
Arabidopsis
Research Center

Aberrant promoter transcripts and heavy methylation are inversely related in two Arabidopsis thaliana transgenic lines displaying variegated silencing of the nptII gene

Morten C. Eike, Inderjit S. Mercy and Reidunn B. Aalen

Our research group is working with a collection of transgenic *Arabidopsis thaliana* lines with single-copy T-DNA insertions, where the *nptII* gene (encoding kanamycin-resistance) is silenced to varying degrees (figure 1). Two of these lines, P4 and P10, show a very high percentage of *nptII*-silencing in the offspring of some of the sibling plants, but little or no silencing in the offspring of other siblings. While P4 plants mostly display type II-III silencing phenotypes, P10 plants display the type I silencing phenotype (figure 1B).

The high variance in silencing between siblings indicates that the onset of silencing in these two lines is a stochastic process involving epigenetic mechanisms. A first choice among approaches was therefore to investigate the methylation status in and around the *nptII* gene.

DNA Methylation

DNA methylation has been associated both with silencing on a transcriptional level (TGS) and with post-transcriptional gene silencing (PTGS) (Fagard and Vaucheret 2000). Using the bisulphite-mediated genomic DNA sequencing method, the methylation status of all cytosine positions in a sequence consisting of the *nos* promoter (*nos*p) and a part of the *nptII* gene (figure 2) were investigated for both lines.

The results (figure 3) show a very high degree of methylation for the silenced siblings, compared to the control lines with little or no silencing. The methylation levels are highest in symmetrical cytosines, but the same variance between silenced and non-silenced siblings is observed also for asymmetrical cytosines (chart 1). The overall level of methylation is higher in line P10 than in line P4: this is probably connected to the different silencing phenotypes observed in these two lines.

When comparing the promoter and transcribed regions (chart 2), a preference for methylation of the former is observed. This indicates that the silencing is mainly on the transcriptional level.

Aberrant RNA

Double-stranded RNA (dsRNA) has been shown to be a potent inducer of silencing in diverse eukaryotic organisms, and has been associated both with PTGS, TGS and DNA methylation of homologous sequences in plants (Matzke, Matzke et al. 2001). The proposed mechanism for this silencing effect involves the processing of the dsRNA into smaller species (21-25 nt), termed small interfering RNAs (siRNAs), which target homologous RNA or DNA for suppression. Double-stranded RNA has long been known to occur in certain RNA viruses, but can also arise from inverted repeats of transgenes or endogenous genes. It has also been hypothesised that dsRNA may be synthesised from single-stranded aberrant RNAs (sense or antisense) by an RNA-dependent RNA polymerase (RdRP) (Wassenegger and Pelissier 1998). However, the evidence for the existence of such transcripts in connection with silencing is scarce.

Using RT-PCR on total RNA isolates (primer positions are given in figure 2), we detected aberrant sense transcripts through the *nos* promoter. Counter to our expectations the transcripts were much more abundant in the siblings showing little or no silencing, compared to the silenced plants (figure 4). The origins of these transcripts have not been determined, but both in line P4 and P10, the T-DNA is positioned upstream of the promoter region of an endogenous gene. Although the endogenous promoters directs transcription the wrong way, several cryptic promoters in the other direction were identified in these areas.

Based on the above theories and observations, our hypothesis is that these transcripts are produced at the same level in all siblings, but that in the silenced plants they are processed into RNA species that target homologous sequences for methylation.

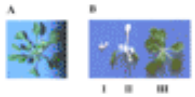

Figure 1 (left): *nptII*-silencing phenotypes. **A**: Km^R phenotype. **B**: *nptII*-silencing (Km^S) phenotypes. Type I: white cotyledonous plants or light green plants with maximum 3-4 leaves; Type II: white plants with deformed, pointed leaves, often with green spots; Type III: larger, green plants with spotted leaves. Depicted plants are 4 weeks old and have been grown on MS-2 Km medium.

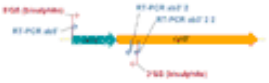

Figure 2 (right): Primers for bisulphite sequencing and RT-PCR. Primers are shown in the *nosp-nptII* construct in the pPCV002 35SGUS-T-DNA. Bisulphite sequencing: 5'GS-7'GS. RT-PCR: RT-reaction. RT-PCR ab/3'.2_2: PCR. RT-PCR ab/3'+RT-PCR ab/3'.2

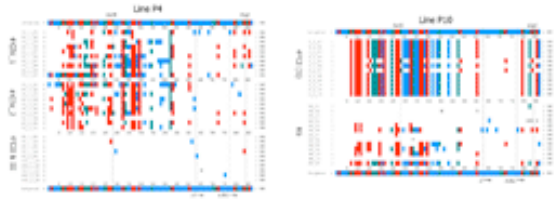

Figure 3: Bisulphite sequencing results. Sequences from 10-13 clones for each sibling line is given. Only the cytosines in the upper strand of the *nosp-nptII* sequence are displayed, and are marked in colour codes corresponding to Chart 1: red and green: symmetrical cytosines (CpG and CpNpG, respectively); blue: asymmetrical cytosines (CpNpN). The transcription start site (+1), the ATG start codon and the restriction sites of two MSRIEs are indicated. Lines with silencing: P4 4'CIV_1 and P4 4'CIV_2 (multiple plants, 100% type II/III silencing), and P10 4'CI (single plant, 83% type I silencing). Controls (little/no silencing): P4 4'CII & III and P10 K6 (multiple plants).

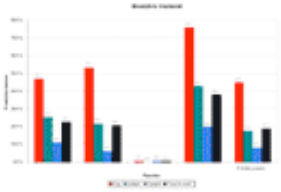

Chart 1: Bisulphite sequencing results: comparison of totals. The represented values are percentages 5'-methylcytosines of the total number of symmetrical (CpG/CpNpG) and/or asymmetrical (CpNpN) cytosines in the *nosp-nptII* sequence. Colour codes are explained in the legend and correspond to figure 3.

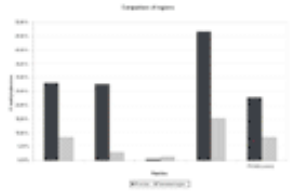

Chart 2: Bisulphite sequencing results: comparison of different regions of the *nosp-nptII* sequence. Represented values are percentages 5'-methyl-cytosines of the total number of symmetrical and/or asymmetrical cytosines in each region.

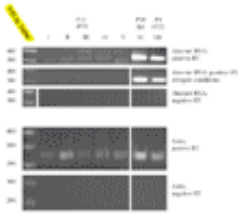

Figure 4: Detection of aberrant RNAs, RT-PCR results. Lane I-V: P10 4'CI, single plants. Lane VI: P10 K6, multiple plants. Lane VII: P4 4'CII, multiple plants. The actin positive and negative controls are shown for comparison. Expected product size is 354 bp for aberrant RNAs, 255 bp for actin mRNA and 540 bp for actin genomic DNA. The weak bands around 540 bp for the P10 4'CI plants disappear under stringent conditions, but cloning and sequencing of a secondary PCR product on the lower band in lane V confirms it as the expected product. Ladder: GeneRuler^{TM} 100 bp DNA ladder, Fermentas

References:

Fagard, M. and H. Vaucheret (2000). "(Trans)gene silencing in plants: How many mechanisms?" Annual Review of Plant Physiology and Plant Molecular Biology 51: 167-194.

Matzke, M. A., A. J. Matzke, et al. (2001). "RNA-based silencing strategies in plants." Curr Opin Genet Dev 11(2): 221-7.

Wassenegger, M. and T. Pelissier (1998). "A model for RNA-mediated gene silencing in higher plants." Plant Mol Biol 37(2): 349-62.

The Benefits and Drawbacks of Hybrid Vehicles in New York City

New York City Diesel-Electric Bus

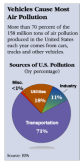

Vehicles are the Primary Cause of Air Pollution

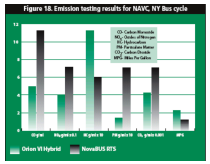

Green: Hybrid Diesel-Electric Bus
Black: Diesel Bus

Benefits of Hybrids

- Lower greenhouse gas emissions than conventional vehicles
- Improved fuel economy
- Enhanced efficiency

Drawbacks

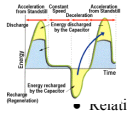

- Relatively short battery life cycle
- Battery disposal
- More expensive than conventional vehicles

4,500 buses in total

- MTA New York City Transit (NYCT) operates
- 200 of these are Orion VII HybriDrive buses
- By 2006 NYCT plans to bring the hybrid-electric fleet to 385 buses

The First Hybrid Gasoline-Electric Models

- 1899: General Electric's four-cylinder gasoline engine hybrid
- 1904: Paris Electric Car Company's Krieger gas-electric hybrid
- 1905: H. Piper filed for patent on hybrid car

Modern Hybrids

- 1997: Toyota's Prius sold in Japan as world's first mass-produced gas-electric hybrid car
- 2000: Honda's Insight hybrid reached U.S. market

1904 Krieger hybrid

Toyota Prius

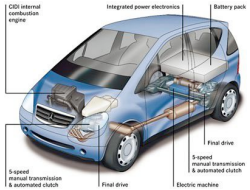

The Mercedes-Benz M-Class HYPER: a hybrid concept vehicle

Maritza Hernandez, Yan Kuznetsov, Nora Nemeth, Melanie Rios, Bola Sim
Professor David J. Szalda
Baruch College

Dental Increment Analysis of *Cebus*

Russell Hogg, CUNY, NYCEP, NYU College of Dentistry

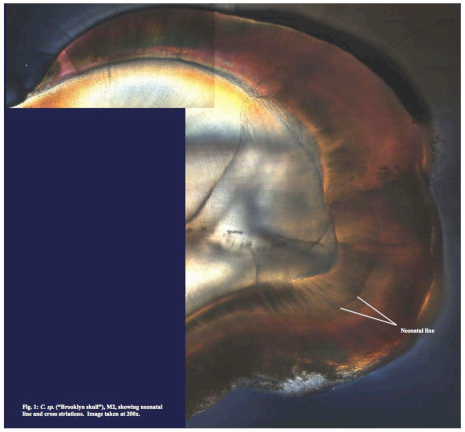

Fig. 1: *C. sp.* ("Brooklyn skull"), M2, showing neonatal line and cross striations. Image taken at 200x.

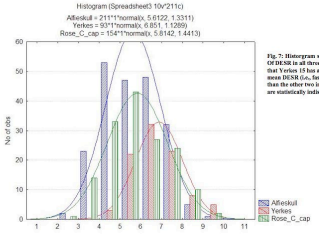

Fig. 7: Histogram showing distributions Of DESR in all three individuals. Note that Yerkes 15 has a significantly higher mean DESR (i.e., faster growth rate) than the other two individuals,which are statistically indistinguishable.

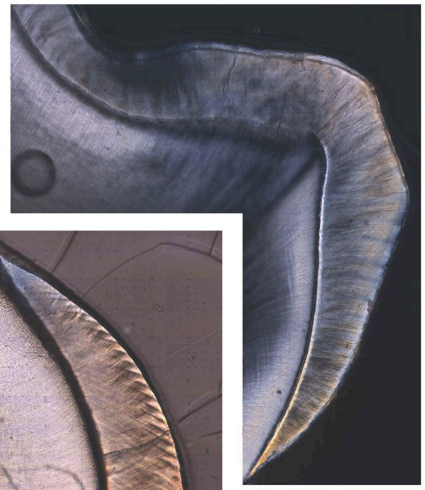

Fig. 4: *C. capucinus* M2, showing both incremental lines And enamel decussation. Observe that decussation is Highest at the occlusal surface, and that Retzius lines again do not extend from the root all the way to the cusps. Image taken at 400x.

Fig. 5: *C. sp.* ("Brooklyn skull") P2. Note clear presence of Retzius lines. Image taken at 200x.

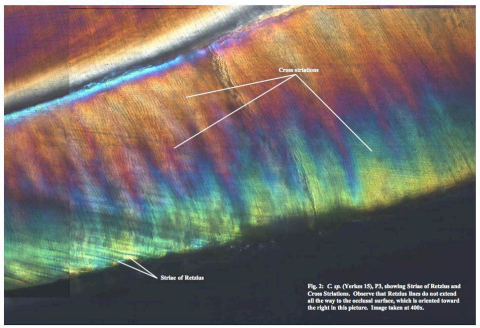

Fig. 2: *C. sp.* (Yerkes 15), P3, showing Striae of Retzius and Cross Striations. Observe that Retzius lines do not extend all the way to the occlusal surface, which is oriented toward the right in this picture. Image taken at 400x.

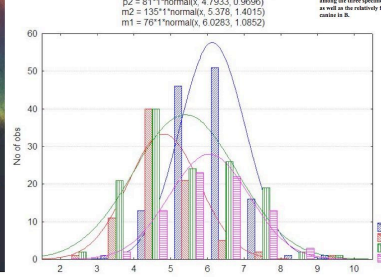

Fig. 8: Differences in enamel secretion rates of individual teeth in A) *C. capucinus*, B) "Brooklyn skull", and C) Yerkes 15.

Note the inconsistent pattern of M2 DESR among the three specimens (faster in A & C), as well as the relatively fast growth of the canine in B.

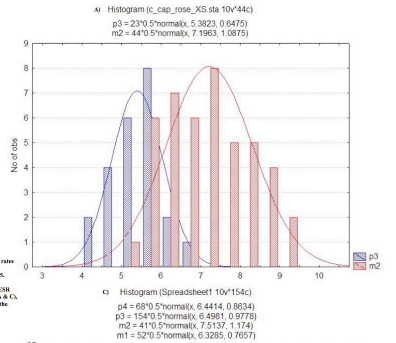

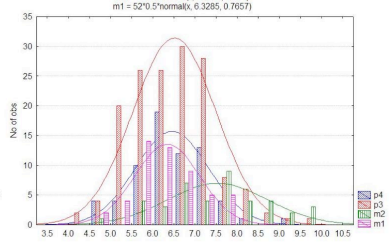

Introduction

In recent years the dentition has seen increased use as a dataset for accessing information on life history variables. Studies such as Dirks (1998), Schwartz *et al.* (2002), and Smith *et al.* (2003) have specifically focused upon enamel microanatomy to reveal direct data on dental growth rates which can be applied to the interrelationships of such factors as phylogeny, ecology, body mass, and brain mass as they impact a taxon's developmental patterns (see also Smith *et al.* 1994, Godfrey *et al.* 2001). To this point the Platyrrhini have been included in such studies in a largely incidental manner, and have received little detailed study.

Therefore, as part of a larger research program on dental microstructure, ecology, and life history in the cebid platyrrhines, this study conducted an analysis of dental microanatomy in capuchin monkeys (*Cebus*). Amongst the platyrrhines, *Cebus* was specifically chosen for this research as it offers unique opportunities for study: 1) it possesses a wide variety of dietary regimes which includes hard-object feeding (and thus serves as an analogue for fossil hominins); 2) possesses a high degree of canine dimorphism which will help "fill out" our understanding of this feature in primates.

Methods

Three individuals of *Cebus* were included for this study: one skeletonized and two preserved in formaline solutions. 1 *C. capucinus* and 1 specimen labeled as *C. apella* were donated from the Rose Primate Collection at Queensborough Community College, CUNY, both zoological specimens. It is this researcher's opinion, however, that the *C. apella* (Yerkes 15) was mislabeled and more likely belongs to *C. olivaceus* based on size and pelage markings. A third specimen of unknown species affiliation (most likely male) was donated by Dr. Alfred Rosenberger.

Teeth were removed from the mandibles of these individuals (dissected out, in the case of the preserved specimens) and incubated in a 5% enzyme solution (Terg-a-zyme®, Alconox) at 45-50 degrees C with daily changes in order to remove the organic matrix and any remaining periodontal tissues. Teeth were then placed in a soxhlet apparatus filled with a mixture of 50% isopropanol and 50% heptane for a week to purge additional organic material; afterward, they were embedded in a poly methyl-methacrylate (PMMA) medium using acetone as a vehicle, and were cured under natural UV light (indirect).

When the PMMA cured to hardness, teeth were sectioned on an Isomet slow-speed diamond wafering saw to a thickness of 200 microns. Sections were mounted on glass slides using the Hard Tissue Research Unit (HTRU) mounting protocol developed by Dr. Haviva Goldman, and were ground to final thickness and polished on a graded series of polishing papers and an Ecomet high-speed buffer (using a 1 micron diamond polish).

All images were collected on a Leica DMRX/E microscope with a JVC digital camera, using a combination of phase-contrast and circularly polarized light. Images were montaged in X-Y axes via an automated stage and Syncroscopy Montage Explorer software. All measurements were calibrated and taken in Syncroscopy Automontage; final images for the poster were edited using Adobe Photoshop. Statistical analyses were performed in Statistica and SPSS.

For all specimens, Daily Enamel Secretion Rates (DESR's) were taken as the mean of cross striations gathered from both cusp and imbricational enamel. Striae of Retzius were summed to indicate overall tooth formation times when available; specimens which did not exhibit Retzius lines in cuspal enamel included an estimate of cusp formation time based upon enamel thickness and the DESR for the cusp. Periodicity for Retzius lines was determined through cross-striation counts and by dividing Retzius breadth by the DESR. All sample preparation and imaging took place at the HTRU facilities of Dr. Timothy Bromage, New York University College of Dentistry, Dept. of Biomaterials and Biomimetics.

Dental Microstructure and Life History

In order to properly access the pertinent developmental information contained within the dentition, one must have: 1) data regarding the relative growth of each individual tooth, and 2) data on the absolute timing of dental events as they correspond to threshold events such as birth and weaning. Histological evidence holds the most promise for minimizing the problems inherent in this type of study by allowing a direct assessment of growth rates in each individual specimen. As pointed out by Boyde (1990), mammalian enamel grows via the apposition of crystalline structures by ameloblast cells. Unlike bone, dental tissues do not undergo further remodeling once they are deposited. Therefore, patterns and anomalies within said tissues stand as permanent markers of an organism's development. Both enamel and dentine contain incremental structures in the form of striations, which represent periodic fluctuations in the rate of enamel deposition (Boyde 1990, Shellis 1998). In the case of the enamel, these structures can be classified into cross-striations in the individual enamel prisms and Striae of Retzius, which cover an entire plane across the cross-striations and represent the surface of the enamel at given times during the crown's development (Boyde 1990, Guatelli-Steinberg 2001). Thus, histological sections of enamel can reveal specific life history information rather like that available in tree rings.

Results

Cebus at the outset appears to have an unusual amount of variety in its Retzius line periodicity, unlike hominoids, which show a consistent seven-day period. Of the three individuals studied, one (*C. sp.*, "Brooklyn skull") showed a period of seven days, while the other two maintained a four-day cycle. In terms of overall DESR, however, the Yerkes15 specimen (*C. apella* / *olivaceus*) is the standout, with a significantly higher growth rate in standard T-tests with a 99% confidence interval; although *C. capucinus* has a higher DESR than the "Brooklyn skull" specimen, they are not statistically distinguishable. Retzius line counts appear to match this pattern, with specimen "Brooklyn skull" taking significantly longer to form an entire P2 tooth crown than Yerkes 15 (653 days vs. 367-434 days, respectively). The matching tooth crown for *C. capucinus* did not possess sufficient morphology to estimate its growth rate, nor did its other premolars.

The canine of specimen "Brooklyn skull" is particularly interesting in light of recent work on the histology of canine sexual dimorphism. Schwartz *et al.* (2005) and Schwartz and Dean (2000) observe that, for anthropoids, canine dimorphism is a result of different timings of growth between males and females rather than rates of enamel/dentine secretion. However, their dataset primarily includes catarrhines (especially hominoids) to the exclusion of platyrrhines. However, the canine for "Brooklyn skull" (a male individual) reflects a significantly higher DESR than the other teeth in its dentition (determined by one-way ANOVA). This implies that for *Cebus*, canine dimorphism results from a different ontogenetic base than for the hominoids. In order to test this hypothesis, female *Cebus* canines will be required to determine whether canines do not grow faster across the board.

It is also worth noting that all three individuals exhibited a high degree of enamel decussation ("gnarling") in occlusal areas, resembling the condition seen in *Paranthropus* (Bromage, pers. comm.; see Figs. 3&4). Decussation is a meandering of the paths of the ameloblast cells that deposit enamel, and creates a series of wavelike patterns in the prisms that help prevent crack propagation. The similarity in *Cebus* and *Paranthropus* is to be expected considering their shared hard-object feeding regime, though from dental wear studies (*e.g.*, Teaford 1985) one would not expect to find this pattern exhibited as strongly as it is in *C. capucinus* specifically (or the Yerkes 15, provided that it does represent *C. olivaceus*). This high amount of decussation obscures Retzius lines in the occlusal areas, and necessitates the use of DESR and enamel thickness to estimate cusp formation times.

Conclusions

Due to the limitations in sampling, all results in this study must be considered preliminary. However, even with only three individuals, *Cebus* has already shown interesting patterns of variation that are not seen in other primates. *Cebus* may hold the key to a revision of theories regarding anthropoid canine dimorphism, and exhibits a high degree of occlusal decussation which was only expected for *C. apella* (which has been shown to follow a much more mechanically demanding diet than other species (Teaford 1985)). The fact that this genus exhibits more variation in its Retzius periodicity than the entire Hominoidea (and possibly the entire Catarrhini) emphasizes the notion that dental growth within the anthropoids (and primates in general) is as of yet poorly understood, and that the Platyrrhini deserve more study.

References

Boyde, A. (1990) Developmental interpretations of dental microstructure. In Rousseau, C.J. (ed.), *Primate Life History and Evolution*. New York: Wiley, pp. 229-267.

Dirks, W. (1998) Histological reconstruction of dental development and age at death in a juvenile gibbon (*Hylobates lar*). *Journal of Human Evolution* 35: 411-425.

Godfrey, L.R., Samonds, K.E., Jungers, W.L., & Sutherland, M.R. (2001) Teeth, Brains, and Primate Life Histories. *American Journal of Physical Anthropology* 114: 192-214.

Guatelli-Steinberg, D. (2001) What can developmental defects of enamel reveal about physiological stress in nonhuman primates? *Evolutionary Anthropology* 10: 138-151.

Schwartz, G.T., & Dean, M.C. (2000) The ontogeny of canine dimorphism in extant hominoids. *American Journal of Physical Anthropology* 115: 269-283.

Schwartz, G.T., Samonds, K.E., Godfrey, L.R., Jungers, W.L., & Simons, E.L. (2002) Dental Microstructure and life history in subfossil Malagasy lemurs. *PNAS* 99: 6124-6129.

Schwartz, G.T., Miller, E.R., & Gunnell, G.F. (2005) Developmental processes and canine dimorphism in primate evolution. *Journal of Human Evolution* 48: 97-103.

Shellis, R.P. (1998) Utilization of periodic markings in enamel to obtain information on tooth growth. *Journal of Human Evolution* 35: 387-400.

Smith, H.B., Crummett, T.L., & Brandt K.L. (1994) Ages of eruption of primate teeth: a compendium for aging individuals and comparing life histories. *Yrbk. Phys. Anth.* 37: 177-231.

Smith, T.M., Martin, L.B., & Leakey, M.G. (2003) Enamel thickness, microstructure and development in *Afropithecus turkanensis*. *Journal of Human Evolution* 44: 283-306.

Teaford, M.F. (1985) Molar microwear and diet in the genus *Cebus*. *American Journal of Physical Anthropology* 66: 363-370.

Acknowledgments

Thanks to Dr. Alfred Rosenberger and Dr. Timothy Bromage for their helpful comments and their time (and specimen access). Thanks also to Dr. Eugene Harris for access to the Rose Primate Collection, and to the kind folks at the Department of Biomaterials and Biomimetics, NYU College of Dentistry. Thanks to Tara Peburn and Terry Capellini for their discussions. This research funded by NYCEP.

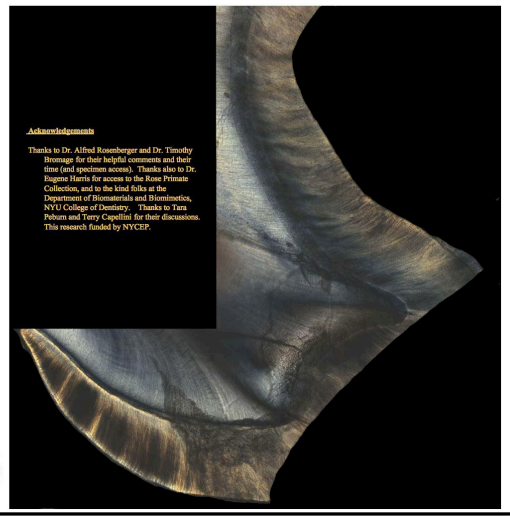

Fig. 6: *C. sp.* ("Brooklyn skull") M1. Note high amount of occlusal wear at Lower left as opposed to Fig. 1, where wear is virtually nonexistant in the same individual. Image taken at 200x.